

# Energy Spectrum of a Honeycomb Lattice under Nonuniform Magnetic Fields

Gi-Yeong OH\*

*Faculty of Liberal Arts and Science, Hankyong National University, Kyonggi 456-749*

(Received 2 March 2006)

The energy spectral properties of an electron in a two-dimensional honeycomb lattice under nonuniform magnetic fields are studied. The dependence of the energy band structures on the strength and the period of the field modulation is elucidated in detail. The effects of the field modulation on the superconducting transition temperature in a wire network with the same geometry is also discussed.

PACS numbers: 73.21.Hb, 73.22.Dj, 73.23.Ad

Keywords: Tight-binding hamiltonian, Hofstadter butterfly, Honeycomb lattice, Superconducting wire network, Effect of magnetic frustration

The electronic properties of two-dimensional (2D) lattices immersed in a uniform transverse magnetic field have been known to be dramatically changed by introducing a nonuniform part in the applied magnetic field [1–9]. For instance, for a square lattice, both the symmetry and the number of subbands in the energy spectrum are modified by introducing a field modulation [1–8]. Besides, for the so-called  $\mathcal{T}_3$  lattice, which is a kind of non-Bravais lattice, not only the energy spectrum but also the localization property of an electronic state is significantly changed by the field modulation - an extremely localized state, called the Aharonov-Bohm cage, becomes delocalized when the field modulation is introduced [9].

However, to date, no study has been done on the effects of nonuniform magnetic fields on the electronic properties of the honeycomb lattice, which is a typical non-Bravais lattice and has attracted renewed attention in connection with carbon nanotubes [10]. Thus, in this paper, we extend the study of field modulation to a honeycomb lattice to elucidate whether or not the effect is in line with the effect in the above-mentioned lattices. To this end, we have calculated the energy spectrum of a honeycomb lattice immersed in a kind of spatially modulated magnetic field. We have also discussed the effects of field modulation on the transition temperature of a superconducting wire network with the same geometry.

The tight-binding electron spectrum of a 2D lattice under a magnetic field can be obtained by solving the following Schrödinger equation:

$$E\psi_i = \sum_j t_{ij} e^{i\gamma_{ij}} \psi_j, \quad (1)$$

where  $t_{ij}$  is the hopping integral between the nearest-

neighboring sites  $i$  and  $j$ , and  $\gamma_{ij} = (2\pi/\phi_0) \int_i^j \vec{A} \cdot d\vec{l}$  is the magnetic phase factor, with  $\phi_0 = hc/e$  being the magnetic flux quantum. For the sake of simplicity, we set  $t_{ij} = 1$  and take the Landau gauge such that the magnetic phase factor along the  $x$  direction in Figure 1 is zero.

Among possible types of modulated fields, we pay attention to a one-dimensional sine-modulated field, where the non-zero  $y$ -component of the vector potential is given by

$$A_y = B_0 x - \frac{B_1 T_x}{2\pi} \cos\left(\frac{2\pi x}{T_x}\right),$$

with  $B_0$  ( $B_1$ ) and  $T_x$  being the uniform (modulated) part of the magnetic field and the period of the modulation along the  $x$  direction, respectively. Denoting the magnetic phase factor along the upward direction on the line

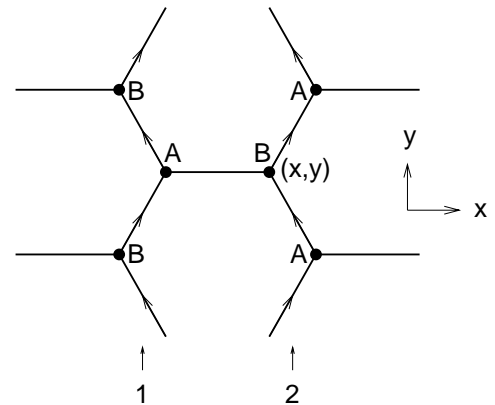


Fig. 1. A portion of a 2D lattice made up of a 2D array of honeycomb unit cells of side  $a$  with atoms at the vertices.

\*E-mail: ogy@hknu.ac.kr

1 (2) in Figure 1 as  $\gamma_{1(2)}$  and using the wave function at site B as  $\psi_B(x, y) = e^{ik_y y} \psi_B(x)$ , we can write Eq. (1) as

$$\begin{aligned} (E^2 - 3) \psi_B(x) &= 2 \cos \left( \gamma_2 + \frac{\sqrt{3}k_y a}{2} \right) \psi_B \left( x + \frac{3a}{2} \right) \\ &+ 2 \cos \left( \gamma_1 + \frac{\sqrt{3}k_y a}{2} \right) \psi_B \left( x - \frac{3a}{2} \right) \\ &+ 2 \cos (2\gamma_2 + \sqrt{3}k_y a) \psi_B(x). \end{aligned} \quad (2)$$

Setting  $\psi_m = \psi_B(x)$  at  $x = 3ma/2$ , Eq. (2) reads

$$\lambda \psi_m = A_{m+1} \psi_{m+1} + C_m \psi_m + A_m \psi_{m-1}, \quad (3)$$

where

$$\lambda = E^2 - 3 \quad (4)$$

and

$$A_m = 2 \cos(\gamma_m + \kappa), \quad C_m = 2 \cos(2\gamma_{m+1} + 2\kappa). \quad (5)$$

Here,  $\gamma_{m(m+1)} = \gamma_{1(2)}$  and  $\kappa = \sqrt{3}k_y a/2$ . Written explicitly,  $\gamma_m$  reads

$$\gamma_m = \pi f \left\{ \left( m - \frac{5}{6} \right) - K \cos \left[ \frac{3\pi a}{T_x} \left( m - \frac{5}{6} \right) \right] \right\}, \quad (6)$$

where  $f = \sqrt{3}B_0 a^2/2$  is the uniform background magnetic flux through the hexagon in units of  $\phi_0$  and

$$K = \frac{2\beta T_x^2}{3\pi^2 a^2} \sin \left( \frac{\pi a}{2T_x} \right),$$

$\beta = B_1/B_0$  being the strength of the field modulation.

A close inspection of Eqs. (3) – (6) for a rational flux  $f = p/q$  with mutual primes  $p$  and  $q$  leads us to write the Bloch condition along the  $x$  direction as

$$\psi_{m+N} = e^{iN\eta} \psi_m, \quad (7)$$

where  $\eta = 3k_x a/2$  and

$$N = \begin{cases} 2T_x q, & T_x \neq 3T'_x \\ 2T'_x q, & T_x = 3T'_x \end{cases},$$

$T'_x$  being an integer. Using Eqs. (3) and (7), we obtain the characteristic matrix as

$$\begin{pmatrix} C_1 & A_2 & 0 & \cdots & A_1 e^{-iN\eta} \\ A_2 & C_2 & A_3 & \cdots & 0 \\ 0 & A_3 & C_3 & \cdots & 0 \\ \vdots & \vdots & \vdots & \ddots & \vdots \\ A_1 e^{iN\eta} & 0 & 0 & \cdots & C_N \end{pmatrix}. \quad (8)$$

Thus, by diagonalizing Eq. (8), we can obtain  $2N$  energy eigenvalues  $\{\pm(3 + \lambda_i)^{1/2}; i = 1, 2, \dots, N\}$  for a given  $\vec{k} = (k_x, k_y)$ .

The energy spectrum of the honeycomb lattice under a uniform magnetic field ( $\beta = 0$ ) has the following symmetries: (i) inversion symmetry about  $E = 0$  for a given

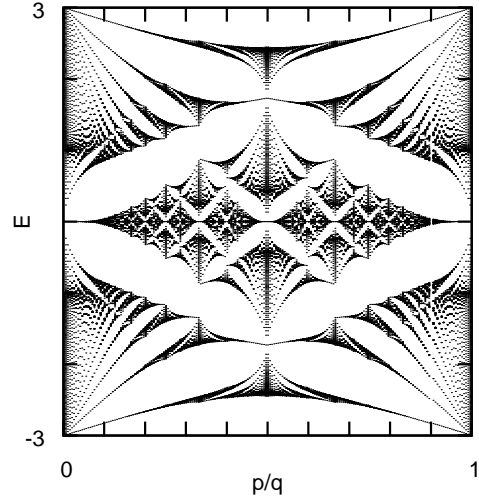


Fig. 2.  $E$  versus  $f = p/q$  under  $\beta = 0$ . In plotting,  $q = 199$  ( $1 \leq p \leq 198$ ) and  $\vec{k} = 0$  are taken into account.

value of  $f$ , (ii) reflection symmetry about  $f = 1/2$  [i.e.,  $E(1-f) = E(f)$ ;  $0 < f < 1/2$ ], and (iii) translational symmetry [i.e.,  $E(1+f) = E(f)$ ]. In addition, the spectrum for a given  $f = p/q$  consists of  $2q$  subbands. However, due to the occurrence of touching between neighboring subbands, the number of distinguishable subbands is less than  $2q$ . For example, for  $f = 1/2$ , touchings between neighboring subbands at  $E = 0$  and  $E = \pm\sqrt{3}$  lead to a single subband structure whose bandwidth is given by  $2\sqrt{6}$ . Similarly, for  $f = 1/3$  (or  $2/3$ ) and  $1/4$  (or  $3/4$ ), due to touching between neighboring subbands at  $E = 0$ , the energy spectra exhibit five and seven subband structures, respectively. We plot in Figure 2 the energy spectrum under  $\beta = 0$  as a function of  $f$ , which is in good agreement with the result of Rammal [11]. In plotting, we took  $q = 199$  ( $1 \leq p \leq 198$ ) and a single  $\vec{k}$  point (i.e.,  $\vec{k} = 0$ ) instead of taking all the  $\vec{k}$ -points in the magnetic Brillouin zone, because the width of every subband for  $q = 199$  is expected to be very small.

With the introduction of a field modulation, two additional parameter  $\beta$  and  $T_x$  play important roles, together with  $f$ , in constructing the energy band structures; the subtle interplay between them leads to band structures that are much more complicated than those without the two additional parameters. One of distinctive effects of the field modulation is a reduction in the symmetries in the energy spectrum; while the inversion symmetry about  $E = 0$  still survives, both the reflection and the translation symmetries appearing under  $\beta = 0$  are broken by introducing a modulation to the magnetic field.

Another effect of the field modulation lies in the change in the widths and the number of subbands in the energy spectrum. Let us first consider a special case: We observe that the band structure for  $f = 1/2$  does not change even when the field modulation is turned on

Table 1. Examples of the number of subbands in the energy spectra for some values of  $f$ ,  $\beta$ , and  $T_x$ .

$f$	1/2	1/3	2/3	1/4	3/4	2/5
$\beta = 0$	1	5	5	7	7	9
$\beta = 0.3, T_x = 2$	1	5	9	7	7	11
$\beta = 0.3, T_x = 3$	1	7	11	7	7	17

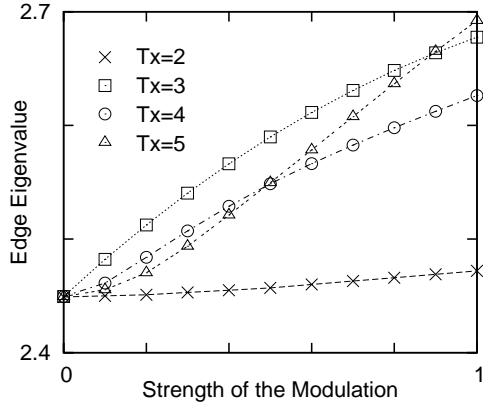


Fig. 3. Top band-edge eigenvalues as functions of the strength of the modulation  $\beta$  for  $f = 1/2$  with several values of  $T_x$ .

- the energy spectrum still has a single subband structure, regardless of  $\beta$  and  $T_x$ . The only effect of the field modulation is to change the width of the subband. For example, the width for  $T_x = 2$  changes monotonically from  $4.898... (= 2\sqrt{6})$  to  $4.944...$  with increasing  $\beta$  from 0 up to 1.0. We plot in Figure 3 the dependence of the top band-edge eigenvalues on  $\beta$  for several values of  $T_x$ , which clearly shows the broadening of the bandwidth.

For generic values of  $f$  except for  $f = 1/2$ , the number, as well as the widths, of the subbands crucially changes, depending on the values of  $T_x$  and  $\beta$ . For example, when  $T_x = 3$ , we observe that the number of subbands for  $f = 1/3$  runs from 5 to 11 with increasing  $\beta$  from 0 to 1: For small  $\beta$  ( $\sim 0.2$ ), the first (fifth) subband of five subbands under  $\beta = 0$  splits into two subbands, resulting in the seven-subband structure. With increasing  $\beta$  ( $\sim 0.3$ ), the second (fourth) subband then splits into two subbands, resulting in the nine-subband structure. With further increases in  $\beta$  ( $\sim 0.6$ ), the third (middle) subband finally splits into three subbands, resulting in the eleven-subband structure. We also observe similar behaviors of subband splitting for other values of  $f$ . Table 1 shows some examples of the number of subbands for several values of  $f$  under  $\beta = 0.3$ . It is worth noting that, while the numbers of subbands for  $f = 1/4$  and  $3/4$  at  $T_x = 2$  and 3 occasionally equal the number of subband under  $\beta = 0$ , the widths of the subbands differ from those under  $\beta = 0$ . In addition, the numbers of subbands become different from one another for other values of  $\beta$ .

Through numerical calculations with various values of

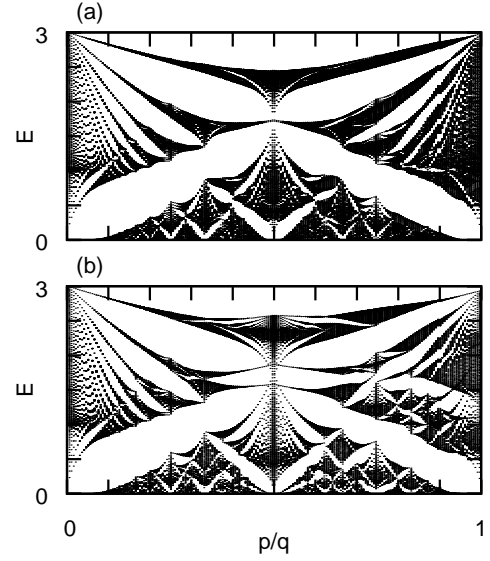


Fig. 4.  $E$  versus  $f$  for  $\beta = 0.3$ : (a)  $T_x = 2$  ( $N = 796$ ) and (b)  $T_x = 3$  ( $N = 398$ ). In plotting,  $q = 199$  ( $1 \leq p \leq 198$ ) and  $\vec{k} = 0$  are taken into account. Due to the inversion symmetry about  $E = 0$ , only the regions of  $E > 0$  are plotted.

$f$ ,  $T_x$ , and  $\beta$ , we found a general trend that the energy spectrum under a modulated magnetic field is considerably darker (*i.e.*, more subbands and fewer subgaps) than that under a uniform magnetic field. Especially, for the widths of the subbands under modulated fields, we found that (i) the width for a given value of  $(T_x, f)$  broadens with increasing  $\beta$ , (ii) the width for a given  $\beta$  broadens with increasing  $N (= 2Tq)$ , and (iii) the width for a given value of  $(\beta, N)$  increases with increasing  $f$ . Figures 4(a) and 4(b) show energy spectra as functions of  $f$  for  $(T_x, \beta) = (2, 0.3)$  and  $(3, 0.3)$ , respectively, where properties (ii) and (iii) can be easily seen. It is worth noting that the appearance of a darker energy spectrum can also be found if one introduces next-nearest-neighbor hoppings in Eq. (1) in a triangular lattice [12].

The transition temperature  $T_c$  of a 2D superconducting wire network under a transverse magnetic field has been known to be intimately related to the edge eigenvalue problem of the corresponding tight-binding electron [13,14], which means that the superconducting wire network may provide a convenient and powerful experimental system where some of the features of the energy spectrum can be observed in realistic conditions. In connection with this, there have been incessant studies on the magnetic behavior of the  $T_c$  of a superconducting honeycomb wire network [15–19]. Here, we extended those studies to investigate the modulation effect on the  $T_c$  of the honeycomb wire network.

Figure 5 shows the curves, indicating a reduction in the  $T_c$ , as a function of  $f$  for  $T_x = 2$  for various values of  $\beta$ . When  $\beta = 0$  (continuous line), the curve is symmetric about  $f = 1/2$ , as expected from the reflection invariance of the energy spectrum. In addition, down-

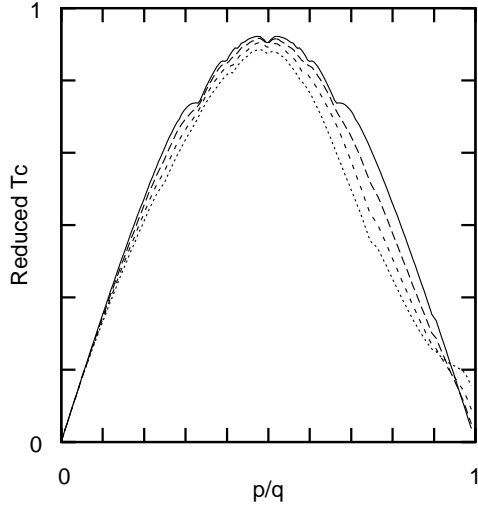


Fig. 5.  $1 - T_c(f)/T_c(0)$  as a function of  $f$  for  $T_x = 2$ . The continuous line is  $\beta = 0$ , the long dashed line is  $\beta = 0.2$ , the short dashed line is  $\beta = 0.4$ , and the dotted line is  $\beta = 0.6$ .

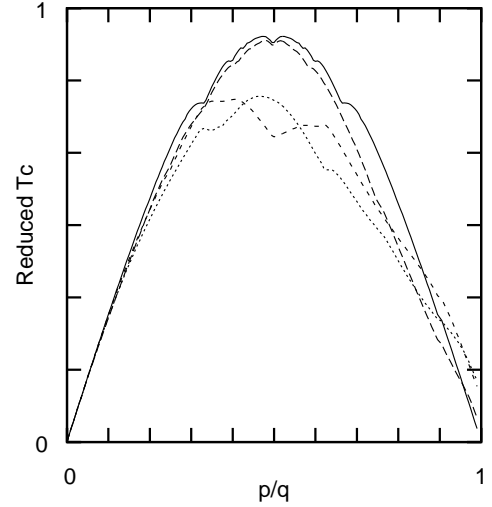


Fig. 6.  $1 - T_c(f)/T_c(0)$  as a function of  $f$ . The continuous line is  $\beta = 0$ , the long dashed line is  $T_x = 2$  and  $\beta = 0.3$ , the short dashed line is  $T_x = 3$  and  $\beta = 0.3$ , and the dotted line is  $T_x = 4$  and  $\beta = 0.3$ .

ward dips at  $f = 1/3, 2/5, 3/7, 1/2, 4/7, 3/5$ , and  $2/3$  are visible, as previously found in Refs. 16-20. The introduction of a field modulation leads to not only a breaking of the symmetry about  $f = 1/2$  but also a smearing out of the dips occurring under  $\beta = 0$ ; the amplitudes of the dips become smaller and eventually disappear with increasing  $\beta$ . Another distinctive feature under modulated magnetic fields is that the reduction in the  $T_c$  (at least, for  $f \leq 0.75$ ) becomes smaller with increasing  $\beta$ , which is in line with a recent report that the decrease in the  $T_c$  in a honeycomb network with a finite size due to a uniform magnetic field is small compared with that in a honeycomb network with an infinite size [19].

The behavior of the  $T_c$  also depends crucially on the period of the field modulation,  $T_x$ . Figure 6 shows the reduced  $T_c$  as a function of  $f$  for various  $T_x$ . It is evident that deformation of the curve obtained for  $\beta = 0$  becomes larger with increasing  $T_x$ . Here, it may be worth making a remark that the maintenance of downward dips for non-zero  $\beta$  indicates that the localization properties of the honeycomb lattice are not changed by introducing a field modulation, unlike the case of  $\mathcal{T}_3$  lattice [9].

In summary, we have studied the energy spectral properties of a two-dimensional honeycomb lattice under sinusoidally modulated magnetic fields and found that not only the symmetry but also the subband structure of the energy spectra undergoes a dramatic change, depending on the parameters  $f$ ,  $\beta$ , and  $T_x$ . We have also investigated the effects of a field modulation on the transition temperature of the superconducting wire network with a honeycomb geometry to show that the modulated part of the magnetic field significantly reduces the effect of frustration due to a uniform magnetic field.

This work was supported by a Korea Research Foundation grant (KRF-2003-015-C00193).

## REFERENCES

- [1] A. Barelli, J. Bellissard and R. Rammal, J. Phys. **51**, 2167 (1990).
- [2] R. R. Gerhardts and D. Pfannkuche, Phys. Rev. B **53**, 9591 (1996).
- [3] A. Y. Rom, Phys. Rev. B **55**, 11025 (1997).
- [4] Q. W. Shi and K. Y. Szeto, Phys. Rev. B **56**, 9251 (1997).
- [5] G. Y. Oh, J. Jang and M. H. Lee, J. Korean Phys. Soc. **29**, 79 (1996); G. Y. Oh, Phys. Rev. B **60**, 1939 (1999).
- [6] M. C. Chang and M. F. Yang, Phys. Rev. B **69**, 115108 (2004).
- [7] Y. Iye, E. Kuramochi, M. Hara, A. Endo and S. Katsumoto, Phys. Rev. B **70**, 144524 (2004).
- [8] M. C. Geisler, J. H. Smet, V. Umansky, K. von Klitzing, B. Naundorf, R. Ketzmerick and H. Schweizer, Phys. Rev. Lett. **92**, 256801 (2004).
- [9] G. Y. Oh, Phys. Rev. B **62**, 4567 (2000).
- [10] See, for example, R. Saito, G. Dresselhaus and M. S. Dresselhaus, *Physical Properties of Carbon Nanotubes* (Imperial College Press, London, 1988) and references therein.
- [11] R. Rammal, J. Phys. **46**, 1345 (1985).
- [12] G. Y. Oh, J. Korean Phys. Soc. **37**, 534 (2000).
- [13] S. Alexander, Phys. Rev. B **27**, 1541 (1983).
- [14] R. Rammal, T. C. Lubensky and G. Toulouse, Phys. Rev. B **27**, 2820 (1983).
- [15] B. Panneiter, J. Chaussy, R. Rammal and J. Villegier, Phys. Rev. Lett. **53**, 1845 (1984).
- [16] S. Teitel and C. Jayaprakash, J. Phys. **46**, L33 (1985).
- [17] Y. Xiao, J. A. Huse, P. M. Chaikin, M. J. Higgins, S. Bhattacharya, and D. Spencer, Phys. Rev. B **65**, 214503 (2002).
- [18] Y. L. Lin and F. Nori, Phys. Rev. B **65**, 214504 (2002).
- [19] O. Sato and M. Kato, Phys. Rev. B **68**, 094509 (2003).